Reconfigurable Grounded Vector Antenna for 3D Electromagnetic Direction Finding Applications

Johan Duplouy, Christophe Morlaas, Hervé Aubert, Philippe Pouliguen, Patrick Potier, Christopher Djoma

Reconfigurable Grounded Vector Antenna for 3D Electromagnetic Direction Finding Applications

Johan Duplouy*†‡, Christophe Morlaas*‡, Hervé Aubert†‡, *Senior Member, IEEE*, Patrick Potier§, Philippe Pouliguen§, and Christopher Djoma§

***Abstract*—In this letter, a reconfigurable grounded wideband antenna is proposed in view of vector sensor applications. This antenna combines two orthogonal and colocated semi-circular arrays of Vivaldi antennas mounted over a metallic support. The radiation patterns of two wideband magnetic dipoles and one wideband electric dipole can be synthesized thanks to an appropriate antenna excitation. Measurement results are in good agreement with the simulated results obtained from full-wave electromagnetic simulations. The proposed antenna exhibits stable radiation patterns over a wide impedance bandwidth of 1.69:1, a high radiation efficiency and a good isolation between the antenna input ports. This antenna is a good candidate for wideband 3D direction finding using a vector sensor.**

***Index Terms*—wideband magnetic and electric dipoles, Vivaldi antennas, vector sensor, direction-of-arrival antenna, reconfigurable antenna.**

I. Introduction

COMPACT direction finding antennas have become very appealing to fulfill the growing demand for widespread civil and defense related applications including wireless communication, radar, radio astronomy, navigation systems and rescue devices [1]. The Direction-of-Arrival (DoA) of an incoming electromagnetic field may be derived from several methods. The classical solution for 2D direction finding uses the spatial distribution of an antenna array [2]. An alternative solution consists of using the polarization diversity arising from the measurement of the six components of the electromagnetic field through a so-called Vector Antenna (VA) [3]. The VA is ideally composed of three electric dipoles and three magnetic dipoles. The design aspects of the VA (including the choice of the constitutive elements) may provide some amplitude and phase distortions on the radiation patterns. In practice, this is usually taken into account thanks to a calibration process (see, e.g., [4]). Nevertheless, the patterns quasi-omnidirectionality in the overall frequency bandwidth is preferred for ensuring accurate estimations of the DoA in all directions. Moreover, high radiation efficiency and stable polarization are required.

Several VA designs have been reported over the past two decades (see, e.g., [5], [6]). However, very few VAs that cover the entire 3D space exist and have recently been reported. An active solution operating at frequencies below 30 MHz was patented in 2013 [7]. It requires power sources for feeding the constitutive active components. In [8], a passive VA placed on a metallic plate is designed for operating in two separate frequencies with narrow bandwidth. To the author's knowledge, no reconfigurable, wideband and passive VA has been reported up to date.

Moreover, while many wideband electric dipoles have been designed (see, e.g., [9]) and could eventually be used for designing wideband VAs, only a few wideband magnetic dipoles have been reported in the literature. In [10], a magnetic dipole using capacitive loading with a Voltage Standing Wave Ratio (VSWR) smaller than 2 over the impedance bandwidth of 1.36:1 is proposed. A printed planar antenna combining four pairs of flag shaped dipoles with parasitic strips was proposed in [11]. This antenna provides an omnidirectional radiation pattern in the E-plane with a reflection coefficient below -10 dB over a 1.52:1 impedance bandwidth. Recently, a circular array of eight tapered slot elements was proposed in [12] for achieving a nearly omnidirectional radiation pattern in the E-plane but with some undesirable ripples within the LTE (Long Term Evolution) band ranging from 1.9 GHz to 2.7 GHz.

In this letter, a reconfigurable wideband VA that synthesizes stable radiation patterns of two magnetic and one electric dipoles is reported for the first time. The measured VSWR on each port is lower than 2.3 over the impedance bandwidth of 1.69:1. These results are obtained from an appropriate choice of the magnitude/phase impressed at the four VA input ports. This VA is composed of two orthogonal and colocated semi-circular array of Vivaldi antennas.

II. Antenna Design

A typical grounded VA for 3D direction finding applications may consist of three colocated orthogonal antennas that measure the x-component and y-component of the magnetic field (H-field) and the z-component of the electric field (E-field) in the Cartesian coordinate system (refer to Fig. 2 for its definition) using two magnetic dipoles and one electric dipole, respectively.

A. Wideband magnetic dipole design

The underlying design principle of a wideband magnetic dipole is to synthesize an omnidirectional radiation pat-

* Ecole Nationale de l'Aviation Civile, TELECOM-EMA, F-31055 Toulouse, France (e-mail: johan.duplouy@enac.fr).
† LAAS-CNRS, Micro and Nanosystems for Wireless Communications Research Group,F-31055 Toulouse, France.
‡ Toulouse University, F-31400 Toulouse, France.
§ Direction Général de l'Armement (DGA), F-75509 Paris, France.

tern in the E-plane over a large frequency range. According to the design methodology reported in [13], the circular array of radius 76.5 mm composed by eight wideband directional radiating elements is expected to achieve a nearly omnidirectional radiation pattern at 3.4 GHz. Fig. 1 gives the derived geometric parameters of a semi-circular array of four Vivaldi antennas mounted over a ground plane. According to the well-documented image theory, the radiation pattern of the grounded array of four Vivaldi antennas is equivalent in the upper half-space to the one of the array of eight Vivaldi antennas. Well-known for exhibiting an endfire directive radiation pattern with moderate gain over a wide bandwidth, Vivaldi antenna presents the two following key features: (1) it radiates a linearly polarized electric field parallel to the plane of the antenna, and (2) it provides a constant beamwidth in the E-plane. As a consequence, Vivaldi antenna is a good candidate for designing the magnetic dipoles of wideband VAs. Parametric studies on l_1, w_1 and the opening rate R (defined in [14]) have been carried out to simultaneously maximize the bandwidth, to minimize the lower frequency of operation f_L and to limit the mid-band amplitude of the VSWR. The higher operating frequency is determined from the undesirable emergence of grating lobes resulting in omnidirectionality defects. Each 50 Ω input port is connected to the 1:2 microstrip line power splitter fabricated using the T-junction. This junction is followed by the impedance transition line to connect the 65 Ω characteristic impedance line to the Vivaldi input port. The slotlines associated with each Vivaldi antenna are electromagnetically coupled through the microstrip-to-slot transition that features the circular cavity and the 80 degrees radial stub in order to broaden the bandwidth [14]. Using $r_c = r_s$, a parametric study has been performed to minimize the lower operating frequency f_L. According to the geometry of the two ports feeding section, the 180° phase differential is applied to obtain the radiation pattern of the magnetic dipole. Vivaldi antennas present an opening rate R of 0.11 mm^{-1} and are printed on a low-cost 0.8 mm thick FR4 substrate (dielectric constant of 4.3 and loss tangent of 0.025). The array is mounted over an octagonal ground plane of side length e. Its dimensions are specified in Table I.

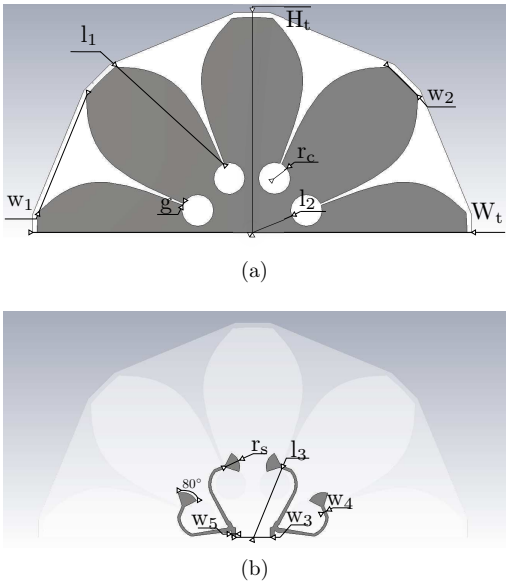

Fig. 1. Topology of the wideband magnetic dipole mounted over a ground plane (not depicted in these figures): (a) Radiating surface and (b) Feeding-section.

TABLE I
Dimensions of the proposed antenna

Parameter	W_t	H_t	w_1	w_2	l_1	l_2	l_3
Value (in mm)	153	76.5	43.8	14.4	50.5	15	26.7
Parameter	g	r_c	r_s	w_3	w_4	w_5	e
Value (in mm)	0.6	5.5	5.5	6.1	1	1.6	125

B. Wideband reconfigurable VA design

The reconfigurable VA topology is depicted in Fig. 2. It consists of two orthogonal and colocated semi-circular arrays of Vivaldi antennas, as previously described. As specified in Table II, the VA enables to shape the radiation pattern of two magnetic and one electric dipoles with an appropriate excitation configuration. The z-component of the electric field is measured by recombining all the input ports in phase, while the x-component and y-component of the magnetic field are measured by using the array positioned along the y-axis (Ports 1 and 2) and the x-axis (Ports 3 and 4), respectively.

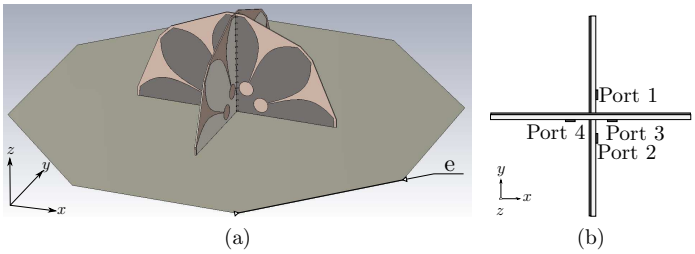

Fig. 2. Topology of the VA: (a) 3D view and (b) Top view.

TABLE II
Amplitude and phase impressed at the four input ports for measuring the field components H_x, H_y and E_z

Configuration	Measured Component	Port 1	Port 2	Port 3	Port 4
1	H_x	1	1∠180°	0	0
2	H_y	0	0	1	1∠180°
3	E_z	1	1	1	1

III. Simulated and Measured Performances

As depicted in Fig. 3, the VA prototype has been manufactured by using the parameters given in Table I. Performances in terms of impedance matching and radiation

properties have been assessed not only through full-wave electromagnetic simulations but also from measurements performed in an anechoic chamber. The measurement of radiation patterns of the wideband magnetic and electric dipoles incorporated in the VA were performed from post-processing, as follows: (1) each port of the antenna was successively fed while the other ports were impedance matched, and four radiation patterns (one pattern per port) were measured; (2) the radiation patterns of the magnetic and electric dipoles were derived from the appropriate recombination of these four patterns (that is, by using the magnitude/phase at the four feeding ports specified in Table II).

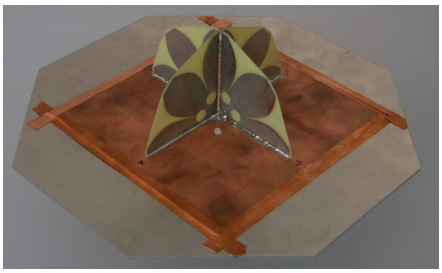

Fig. 3. Photograph of the wideband and reconfigurable VA prototype.

A. Impedance matching

Fig. 4 displays the simulated and measured VSWR of the investigated VA. According to the method used for deriving the radiation patterns given above, only the VSWR at port i ($i \in [\![1,4]\!]$) is considered here by using the classical S-parameters definition. Furthermore, only the simulated VSWR at port 1 is plotted for symmetry reasons. The simulated and measured impedance bandwidths (for a VSWR smaller than 2.3) are respectively of 1.71:1 from 2.08 GHz to 3.56 GHz and of 1.69:1 from 2.10 GHz to 3.55 GHz. A good agreement is obtained between the simulated and measured results. The slightly discrepancy between the measured VSWR can be attributed to manufacturing imperfections. Moreover, the redesign of the feeding section (T-junctions and impedance transition lines) would be useful to improve the VSWR at 2.8 GHz. The VA is included in a half-sphere within a $0.52\lambda_0$ radius, where λ_0 is the free space wavelength at 2.10 GHz.

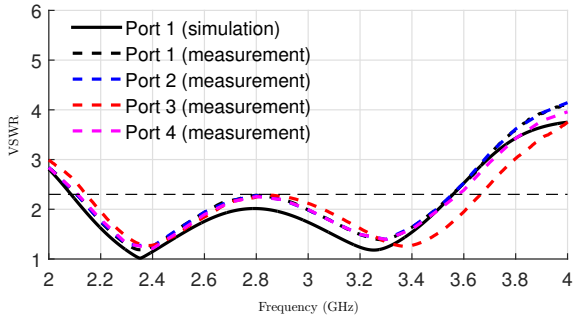

Fig. 4. Simulated and measured VSWR of the proposed VA.

Fig. 5 shows the measured isolation between port 1 and the three other ports of the VA. The measured isolation S_{1j} ($j \in [\![2,4]\!]$) corresponds to the standard case where the ports 1 and j are connected to the vector network analyzer while the other ports are impedance matched. It can be observed that the mutual coupling between the port 1 and the other ports does not exceed -23 dB over the operating bandwidth. Furthermore, the same level of isolation is obtained at the other ports.

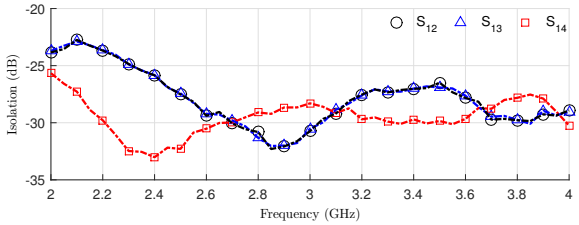

Fig. 5. Measured isolation between port 1 and the other three ports of the proposed VA.

B. Radiation properties

The same octagonal ground plane was used for both electromagnetic simulation and measurements. Moreover, simulation results with an infinite ground plane are also given here in order to analyze the impact of the finite ground plane on radiation characteristics.

Fig. 6 presents the simulated and measured gains in the yz-plane for the first and third configurations of Table II at several frequencies in the bandwidth. The recombined radiation patterns are similar to ones of the magnetic and electric dipoles in the E-plane. It can be noted from Figs. 6(a-c-e) that the radiation pattern of the first configuration is quasi-omnidirectional with some undesirable ripples that can be attributed to the effect of the finite size of the ground plane. Indeed, an omnidirectional radiation pattern in the E-plane (with some ripples lower than 2 dB over the entire bandwidth) is achieved with the infinite ground plane. As frequency increases, it can be observed from Figs. 6(b-d-f) that undesirable blind directions appear in the radiation pattern of the third configuration when then VA is mounted over an infinite ground plane in the direction θ close to 70° (for $\phi \in \{0°, 90°, 180°, 270°\}$). For the finite-sized ground plane, this null is advantageously replaced by non-zero values of the gain.

Fig. 7 shows the simulated gain in the xy-plane for the first and third configurations of Table II at several frequencies in the operating bandwidth. The synthesized radiation patterns are close to ones of magnetic and electric dipoles in the H-plane. The radiation pattern of the electric dipole presents some ripples in the H-plane at higher frequencies.

Fig. 8 presents the simulated total efficiency of the VA mounted over the octagonal ground plane using different operating modes. The simulated total efficiencies of the different operating modes exceed 80% over the entire bandwidth.

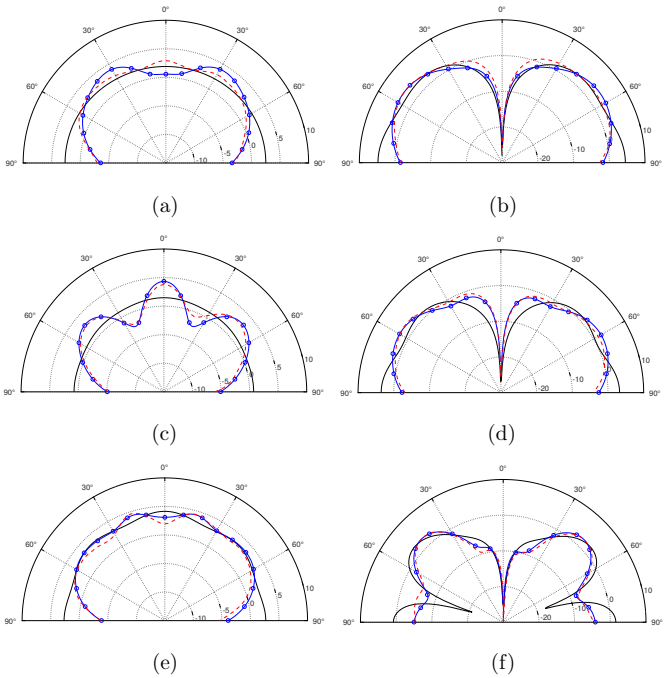

Fig. 6. Simulated and measured realized gain in co-polarization and in the yz-plane of the Config. 1 (left figures) and the Config. 2 (right figures) of Table II at: (a) & (b) 2.2 GHz, (c) & (d) 2.8 GHz, and (e) & (f) 3.4 GHz. The black line is the simulated radiation pattern with an infinite ground plane. The blue circle-marked line and the red dashed line are the simulated and measured radiation pattern with the same finite ground plane, respectively.

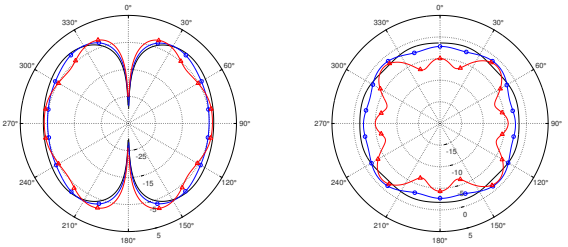

Fig. 7. Simulated realized gain in the xy-plane in co-polarization at several frequencies in the bandwidth of (a) the Config. 1 and (b) the Config. 3 of Table II when the VA is mounted on a finite ground plane. The black line, the blue circle-marked line and the red triangle-marked line correspond to the radiation patterns at 2.2 GHz, 2.8 GHz and 3.4 GHz, respectively.

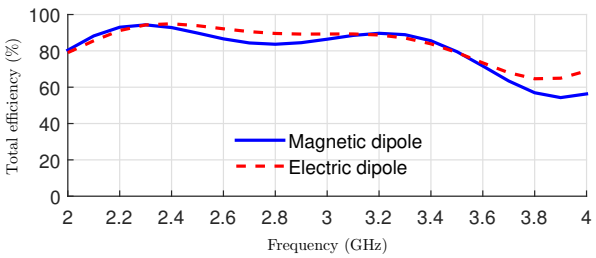

Fig. 8. Simulated total efficiency of the VA mounted over a finite ground plane for its different operating modes.

IV. Conclusion

A reconfigurable grounded VA for 3D direction finding has been presented in this letter. The proposed VA takes advantage of only two semi-circular arrays of Vivaldi antennas to synthesize, over a 1.69:1 bandwidth, the radiation patterns of two magnetic dipoles and one electric monopole with an appropriate control of the excitation. A prototype of this antenna was manufactured and experimentally characterized. A good agreement between the experimental results and the simulation results was obtained. The VA presents a good isolation between its ports (lower than -23 dB) and a high radiation efficiency. The prototype is included in a half-sphere within a $0.52\lambda_0$ radius, where λ_0 is the free space wavelength at the lowest operating frequency. Early results of the direction finding performances of this VA are very encouraging and will be presented in a future paper. This antenna has been designed for direction finding applications, but it could also be used for reconfigurable antenna applications as well as for MIMO (Multiple Input Multiple Output) applications.

Acknowledgment

The authors acknowledge the French Defense Agency (Direction Général de l'Armement, DGA) and the Occitanie regional council for their financial support.

References

[1] T. E. Tuncer and B. Friedlander, *Classical and Modern Direction-of-Arrival Estimation*. Academic Press, 2009.

[2] P. Gething, *Radio Direction Finding and Superresolution*, ser. Electromagnetics and Radar Series. P. Peregrinus, 1991.

[3] A. Nehorai and E. Paldi, "Vector-sensor array processing for electromagnetic source localization," *IEEE Transactions on Signal Processing*, vol. 42, no. 2, pp. 376–398, Feb 1994.

[4] S. Chandran, *Advances in Direction-of-arrival Estimation*. Artech House, 2005.

[5] L. L. Monte, B. Elnour, and D. Erricolo, "Distributed 6D vector antennas design for direction of arrival applications," in *International Conference on Electromagnetics in Advanced Applications*, Sept 2007, pp. 431–434.

[6] M. J. Slater, C. D. Schmitz, M. D. Anderson, D. L. Jones, and J. T. Bernhard, "Demonstration of an electrically small antenna array for UHF direction-of-arrival estimation," *IEEE Transactions on Antennas and Propagation*, vol. 61, no. 3, pp. 1371–1377, March 2013.

[7] B. Almog, "Compact 3D direction finder," Patent, Mar, 2013, EP20120184835.

[8] J. Lominé, C. Morlaas, C. Imbert, and H. Aubert, "Dual-band vector sensor for direction of arrival estimation of incoming electromagnetic waves," *IEEE Transactions on Antennas and Propagation*, vol. 63, no. 8, pp. 3662–3671, Aug 2015.

[9] M. Li and N. Behdad, "A compact, capacitively fed UWB antenna with monopole-like radiation characteristics," *IEEE Transactions on Antennas and Propagation*, vol. 65, no. 3, pp. 1026–1037, March 2017.

[10] K. Wei, Z. Zhang, and Z. Feng, "Design of a wideband horizontally polarized omnidirectional printed loop antenna," *IEEE Antennas and Wireless Propagation Letters*, vol. 11, pp. 49–52, 2012.

[11] Y. Yu, F. Jolani, and Z. Chen, "A wideband omnidirectional horizontally polarized antenna for 4G LTE applications," *IEEE Antennas and Wireless Propagation Letters*, vol. 12, pp. 686–689, 2013.

[12] T. S. P. See, X. Qing, and Z. N. Chen, "A wideband horizontally polarized omnidirectional antenna," in *IEEE 4th Asia-Pacific Conference on Antennas and Propagation*, June 2015, pp. 294–295.

[13] T. S. Chu, "On the use of uniform circular arrays to obtain omnidirectional patterns," *IRE Transactions on Antennas and Propagation*, vol. 7, no. 4, pp. 436–438, October 1959.

[14] J. Shin and D. H. Schaubert, "A parameter study of stripline-fed vivaldi notch-antenna arrays," *IEEE Transactions on Antennas and Propagation*, vol. 47, no. 5, pp. 879–886, May 1999.